TU Delft

Delft University of Technology

A new hermetic sealing method for ceramic package using nanosilver sintering technology

Zhang, Hao; Liu, Yang; Wang, Lingen; Fan, Jiajie; Fan, Xuejun; Sun, Fenglian; Zhang, Guo Qi

DOI
10.1016/j.microrel.2017.12.030

Publication date
2018

Document Version
Accepted author manuscript

Published in
Microelectronics Reliability

Citation (APA)
Zhang, H., Liu, Y., Wang, L., Fan, J., Fan, X., Sun, F., & Zhang, G. Q. (2018). A new hermetic sealing method for ceramic package using nanosilver sintering technology. *Microelectronics Reliability*, *81*, 143-149. https://doi.org/10.1016/j.microrel.2017.12.030

Important note
To cite this publication, please use the final published version (if applicable).
Please check the document version above.

Copyright
Other than for strictly personal use, it is not permitted to download, forward or distribute the text or part of it, without the consent of the author(s) and/or copyright holder(s), unless the work is under an open content license such as Creative Commons.

Takedown policy
Please contact us and provide details if you believe this document breaches copyrights.
We will remove access to the work immediately and investigate your claim.

This work is downloaded from Delft University of Technology.
For technical reasons the number of authors shown on this cover page is limited to a maximum of 10.

© 2018 Manuscript version made available under CC-BY-NC-ND 4.0 license https://creativecommons.org/licenses/by-nc-nd/4.0/

A new hermetic sealing method for ceramic package using nanosilver sintering technology

Hao Zhang[1, 2, 3*], Yang Liu[3], Lingen Wang[4], Jiajie Fan[1, 2, 5], Xuejun Fan[1, 6], Fenglian Sun[3], Guoqi Zhang[1, 7]

[1]Changzhou Institute of Technology Research for Solid State Lighting, 213161, Changzhou, China
[2]Beijing Research Center, Delft University of Technology, Beijing, China
[3]Harbin University of Science and Technology, 150040, Harbin, China
[4]Boschman Technologies B.V., 6921EX, Duiven, Netherlands
[5]College of Mechanical and Electrical Engineering, Hohai University, 213022, Changzhou, China
[6]Department of Mechanical Engineering, Lamar University, Beaumont, TX77710, USA
[7]EEMCS Faculty, Delft University of Technology, 2628CD, Delft, the Netherlands
* Corresponding author: Hao Zhang (Email: hoayzhang@163.com)

Abstract

High reliable packaging materials are needed for electronics when they work at harsh environments. Among which, the nanosilver material has been widely studied and applied in power electronics due to its low processing temperature and high reliability. This paper investigates the bonding properties of nanosilver sintered hermetic cavity. There are two kinds of lids used in this study, including copper lid and silicon lid. The X-Ray and C-Mode Scanning Acoustic Microscopy (C-SAM) results revealed that delamination tended to happen in Cu lid sintered cavity as the recovery of deformed Cu lid was hindered by sintered dense Ag layer. However, no delamination or cracks were found in Si lid sintered cavity. Finite element analysis (FEA) method was used to investigate the effects of lid materials on the stress distribution of lid. The results indicated that the Cu lid sintered cavity showed a much higher stress than the Si lid sintered cavity under the sintering parameters of 250°C and 10 MPa. There is no obvious change in the stress distribution areas on Cu lid with the increasing of pressures from 5 to 30 MPa. However, the distribution area of stress on Si lid expanded obviously only when the sintering pressure increased to 30 MPa. With the increase of sintering pressures from 5 to 30 MPa, the maximum stresses on Cu lid are almost the same, while increasing trend was found on Si lid.

Keywords: harsh environments, nanosilver, sintered, lid, stress

1. Introduction

Electronics, operating at harsh environment, are usually suffering extremely high/low temperature shock and high pressure, when they are applied in the area of renewable energy, aerospace engine, oil and gas drilling and production [1-4]. Some of these electronics need to be hermetically sealed to prevent the deterioration of function and reliability.

The hermeticity is usually achieved by using various sealing methods, such as

thermocompression bonding [5-7], soldering [8-10], glass frit bonding [11, 12], seam welding [13] and anodic bonding [14, 15]. Among these methods, the Au-Sn eutectic soldering technology is one of the widely used hermetic seal methods due to its favorable mechanical strength, flux-free process, and hermeticity [16, 17]. Zhang *et al* [18] designed an electrical test method to monitor the bonding quality of AuSn eutectic soldered micro-electro-mechanical systems (MEMS) cavities. They found that the sample with a lower resistivity owned a thicker $(Au, Ni)_3Sn_2$ phase at the bonding interface and a lower bonding strength. Demir *et al* [19] fabricated the thermal evaporated Au and Sn layers as a seal ring in MEMS cavity. The bonding was achieved by the formation of Au-Sn intermetallic compounds (IMC) and the average shear strength can reach 23 MPa. Rautiainen *et al* [16] used the Au-Sn seal ring for bonding silicon wafers and caps through solid–liquid interdiffusion (SLID) method. The bonded wafers with Ni layer between the TiW adhesion layer showed quite high shear strength while voids were found at the shear and tensile fracture surface.

However, the processing temperature (over 300°C) of Au-Sn eutectic solder is quite high, which may introduce the thermal induced stress concentration and damage in the electronic components. Although the Au-Sn stacked metal layers in SLID method can be processed at temperatures around 235°C, the complicated deposition procedure and processing technology limit its further application. Furthermore, the excessive growth of IMC may decrease the bonding strength of joint because of its brittle nature [20, 21]. In addition, the cost of Au-Sn eutectic alloy is also quite high. So there is an urgent need for developing a new sealing material that can work steadily at harsh environments.

Recently, the nanosilver sintering technology has attracted a lot of attention in the die attach process of power semiconductor fields. This process can be achieved at low temperature around 250°C and served at relative high environment temperatures over 200°C [22, 23]. Comparing with the traditional Au-Sn eutectic soldering method, the nanosilver sintering technology offers relatively lower processing temperature and higher reliability. Until now, there are few publications report the application of nanosilver sintering technology in hermetic sealing process.

This paper investigated the bonding properties of nanosilver sintered hermetic cavity. The bonding qualities of sintered Ag layer were analyzed by using X-Ray and C-SAM imaging methods. The effects of lid materials and sintering pressure on the stress distribution of sintered cavity were investigated by FEA method.

2. Experiments

2.1 Sample preparation

The ceramic cavity (Al_2O_3) with a gold (Au) coating layer (10 μm) on the top surface was used in this paper. The sealing material was nanosilver film (Ag film), which has a thickness of 65 μm (from Alpha Assembly Solutions). The Ag film was cut by laser into hollow square shape with a width of 0.22 mm according to the sealing area on the top surface of the cavity. There are two kinds of lids used in this study, including copper (Cu) and silicon (Si) based ones. Both two kinds of lids were

coated with silver on the top surface of sealing area. The materials are shown in Fig. 1.

The whole manufacture process includes two steps: firstly, the Ag film cut by laser was laminated on the gold layer of the cavity at 130°C for 2 min with a pressure of 5 MPa. Secondly, the lid was assembled on the laminated cavity and then the whole cavity was placed in the mold inside of the sintering equipment. Note that the lid was placed on the bottom side and the cavity was placed on the top side. The whole cavity was then directly sintered at 250°C for 5 min by a precisely controlled and monitored system from Boschman Technologies. The sintering process was achieved at the atmosphere. In order to get a dense microstructure and high mechanical strength, a pressure of 10 MPa was applied through the dynamic insert during the sintering process. This dynamic insert can help to ensure a uniform pressure through a real time feedback system. After sintering, the package was cooled down to room temperature at the atmosphere for 3 min. The sintering equipment and the two processing steps were shown in Fig. 1.

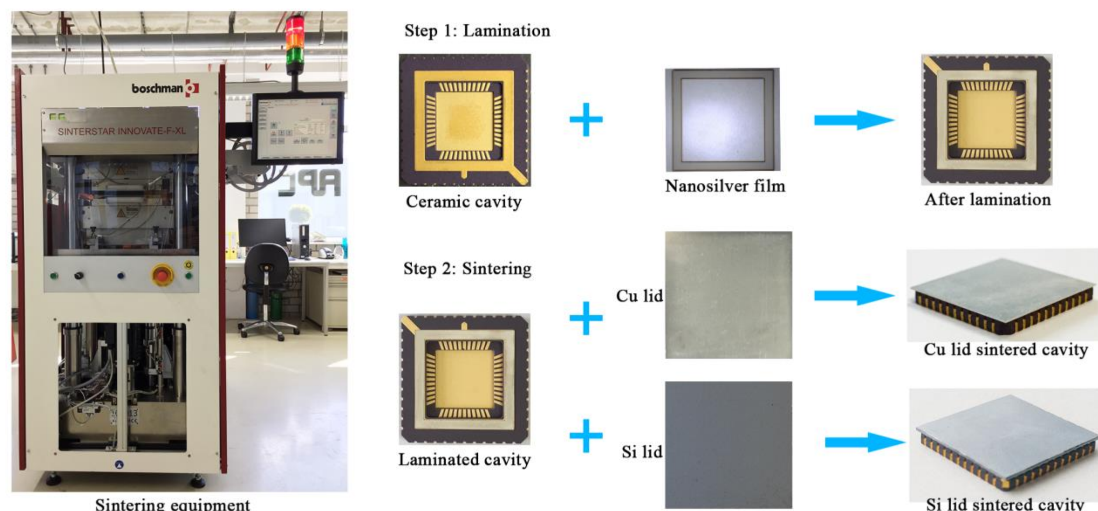

Fig. 1. Sintering equipment and sample preparation

After sintering, the sample was taken out from the equipment and cooled down to room temperature. The sintered cavity was further detected in X-Ray imaging system to check the cracks in the bonding layer. The sintered cavity was also examined through C-SAM test to determine whether delamination existed or not. Finally, the bonding quality of nanosilver sintered cavity was evaluated through the captured images in the two tests.

2.2 Finite element analysis method

The FEA method was used in this paper to determine the residual stress in the sintered cavity during sintering process. Some assumptions are applied to the 3D model to save computational time without affecting the accuracy of the solution:

- The 3D model was regarded as a symmetrical one, so only a quarter of the model was built for simulation.

- The surface coatings on the Cu and Si lid were neglected in the 3D model.

- The sintered silver layer was considered as a uniform and constant material.

The structure of the cavity is shown in Fig. 2, it consists of four layers: lid (Cu or Si), sintered Ag layer, Au coating and cavity (Al_2O_3). During simulation, the package was first heated up to 250°C from room temperature within 1 min and then kept at 250°C for 5 min. Then the package was cooled down to room temperature within 3 min. The sintering pressure of 5 (or 10, 20, 30) MPa was applied on the back side of the cavity during heating and sintering. The large deflection function was turned on to better predict the deformation of lid. The general material properties that are used for simulation were summarized in Tab. 1.

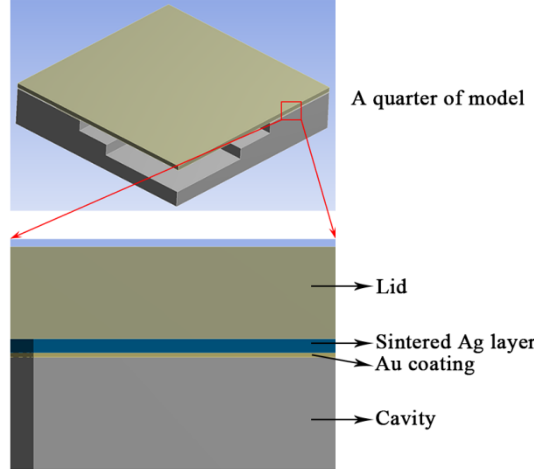

Fig. 2. 3D structure of a quarter model for simulation

Since the processing temperature is quite high, so the elastic-plastic models are applied for sintered Ag layer and Cu lid. The Garofalo law is a time dependent model, which describes the function between stress and temperature with a sine hyperbolic creep law was used for sintered Ag layer, can be expressed in equation 1 [24]:

$$\dot{\varepsilon} = \mathrm{A} \cdot [\sinh(\alpha \cdot \sigma)]^n \cdot exp\left(\frac{-E_a}{R \cdot T}\right) \quad (1)$$

where $\dot{\varepsilon}$ is the steady state creep rate, σ is the stress in MPa, R the universal gas constant and T is the temperature in K, the other four constants A, α, n, E_a are defined in Tab. 2.

The Chaboche model was used to describe the nonlinear kinematic hardening behavior of the Cu lid. The yield function of Chaboche model can be expressed as equation 2 [25, 26]:

$$F = \sqrt{\frac{3}{2}(s-\alpha)(s-\alpha)} - Y = 0 \quad (2)$$

where s is the deviator stress, α is the back stress and Y is the yield stress of material.

The back stress α in the Chaboche model can be described as equation 3:

$$\alpha = \sum_{i=1}^{n} \alpha_i \quad (3)$$

$$\Delta\alpha_i = \frac{2}{3} C_i \cdot \Delta\varepsilon^{pl} - \gamma_i \alpha_i \cdot \Delta\hat{\varepsilon}^{pl} + \frac{1}{C_i}\frac{dC_i}{d\theta}\Delta\theta \cdot \alpha \quad (4)$$

where ε^{pl} represents the accumulated plastic strain, θ represents the temperature, C_i

and γ_i are the material parameters in Chaboche model, C_i represents the initial hardening modulus, the decreasing rate of hardening modulus with the increase of plastic strain is controlled by γ_i, i represents the number of kinematic models, here i = 1, 2. The parameters of Chaboche model for Cu lid is given in Tab. 3, and the yield stress of Cu that varies with temperature is described in Tab. 4.

Tab. 1 Material properties adopted in simulation [24, 27-29]

Material	Length (mm)	Width (mm)	Thickness (mm)	Young's modulus (GPa)	Poisson ratio	CTE (10^{-6} K^{-1})
Si	16.5	16.5	0.52	130.8	0.28	4.2
Cu	16.5	16.5	0.2	110	0.34	17
Sintered Ag	-	0.22	0.03	23°C, 32	0.25	20.3
				100°C, 22		
				200°C, 12		
Au	-	0.22	0.01	80	0.30	14
Al_2O_3	16.5	16.5	1.645	370	0.22	6.8

Tab. 2 Constants for Garofalo law [24]

Material	A (s^{-1})	α (MPa^{-1})	n	E_a (kJ ·mol-1)
Sintered Ag	0.12	0.25	0.9	55.04

Tab. 3 Parameters for Chaboche model of Cu [25]

Temperature (°C)	C_1 (MPa)	γ_1	C_2 (MPa)	γ_2
20	54041	962	721	1.1
50	52880	1000	700	1.1
150	45760	1100	600	1.1
250	38040	1300	400	10

Tab. 4 Yield stress of Cu at various temperatures [26]

Material	20°C	50°C	150°C	250°C
Cu	210 MPa	208 MPa	201 MPa	170 MPa

3. Results and discussion

3.1 Evaluation of bonding quality

The X-Ray and C-SAM tests were conducted to the sintered cavities, and the results are shown in Fig. 3. The dark hollow square in the X-Ray image represents the sintered Ag layer, and the corresponding area can be seen in C-SAM image. Fig. 3. (a) is the Cu lid sintered cavity, and the image in the middle is the partial enlarged view of bottom right corner. Based on the test results, it can be seen that there is no crack observed in the sintered Ag layer in Cu lid sintered cavity. However, the sintered Ag layer is not flat and it is not continuously connected in the horizontal direction. This result indicates that delamination is quite serious in the sintered Ag layer with Cu lid and it will result in a weak bonding between the Cu lid and cavity. In the contrast, the sintered Ag layer in Si lid sintered cavity is quite smooth and flat, as shown in Fig. 3. (b). There is no visible crack or delamination inside the sintered Ag layer, which implies a good bonding between the Si lid and cavity.

In the sintering process, the temperature rose to 250°C within dozens of seconds. The Cu lid deformed with temperature rising, and the applied pressure (10 MPa) made the deformation even more serious. During which, the nanosilver particles inside the film began to coalesce with adjacent particles and formed a relatively dense microstructure. This sintered Ag layer has a high Young's modulus and hindered the recovery of deformed Cu lid in the cooling process. Meanwhile, certain stress was also induced in the sintered Ag layer and weakened the bonding quality, and finally resulted in the delamination. However, since the Si lid has a much lower CTE than the Cu lid, less residual stress was generated in Si lid during sintering process when compared to the Cu lid. What's more, the thickness of Cu lid was thinner than the Si lid, which also contributed to the high stress in Cu lid. Hence, the nanosilver sintered Si lid cavity has a better bonding quality than the Cu lid sintered one. In order to further verify the test results, the FEA method was used to simulate the residual stress resulted from the sintering process.

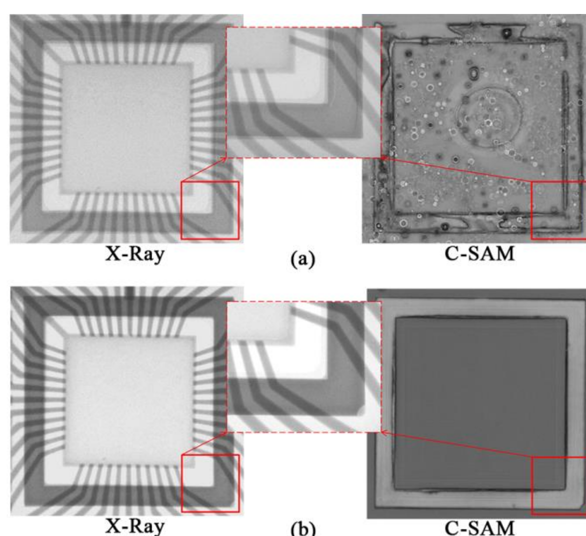

Fig. 3. X-Ray and C-SAM images of nanosilver sintered cavities, (a) Cu lid and (b) Si lid

3.2 Effects of lid material on the stress distribution of sintered cavity

In order to furtherly understand how the lid material affects the sintering quality in the sealed cavity bonded by nanosilver, the FEA method was applied to simulate the residual stress distribution in the sintered cavity during sintering process. The Von Misses stress distributions of Cu lid and Si lid sintered cavities after sintering are shown in Fig. 4 and Fig. 5, respectively. As shown in Fig. 4 (a), the stress concentration tends to happen in the central part of the Cu lid, and the outer corner area of Cu lid exhibits the lowest stress level. By combining Fig. 4. (b), (c), (d) and (e), the maximum stress of 196.47 MPa is determined, which locates along the two sides of sintered Ag layer. The sintered Ag layer also has a quite high stress about 109.16 MPa around the outer corner area and delamination tends to occur at this area, as shown in Fig. 4 (d). What's more, the central part of sintered Ag layer at each side gains the relative low stress and will not greatly decrease the bonding quality of sintered Ag layer. Those results have a good agreement with the X-Ray and C-SAM results in Fig. 3. Since the cavity is ceramic (Al_2O_3) based material, only 65.50 MPa maximum stress is generated because of the high Young's modulus of itself, as seen in Fig. 4 (e).

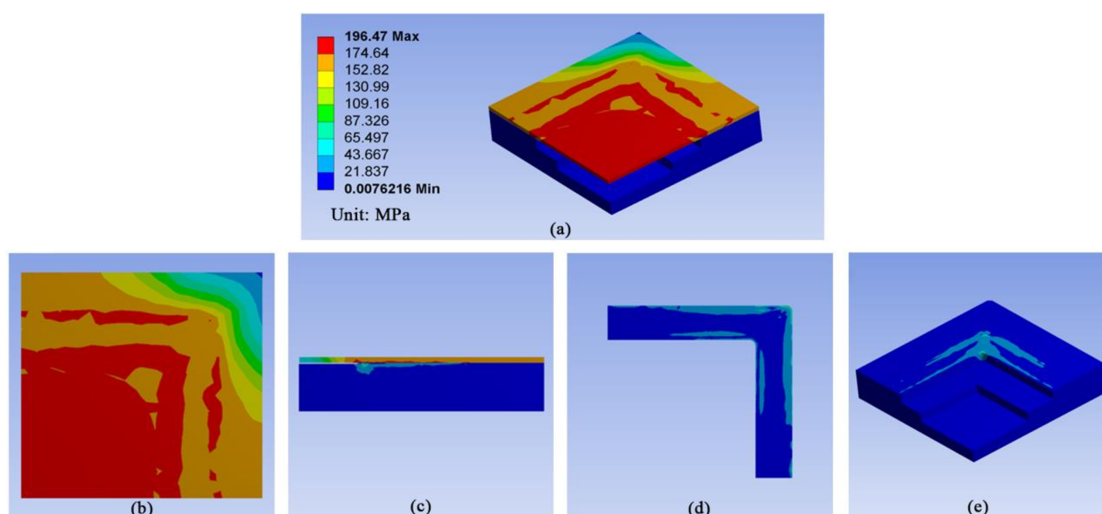

Fig. 4. Stress distribution of Cu lid sintered cavity, (a) 3D model, (b) top view of Cu lid, (c) cross sectional view of 3D model, (d) top view of sintered Ag layer and (e) 3D view of cavity

While in the Si lid sintered cavity, the stress concentration mainly locates on the corner area of sintered Ag layer on Si lid, as shown in Fig. 5 (a). According to the simulation results in Fig. 5 (b), (c), (d) and (e), the maximum stress of 26.19 MPa is generated on the top surface of the Si lid and the area of the outer corner of sintered Ag layer. Except the four stress concentration corner areas on Si lid, relative low stress distributes on the whole lid. Similar results are also found in the sintered Ag layer in Fig. 5 (d) and the cavity in Fig. 5 (e).

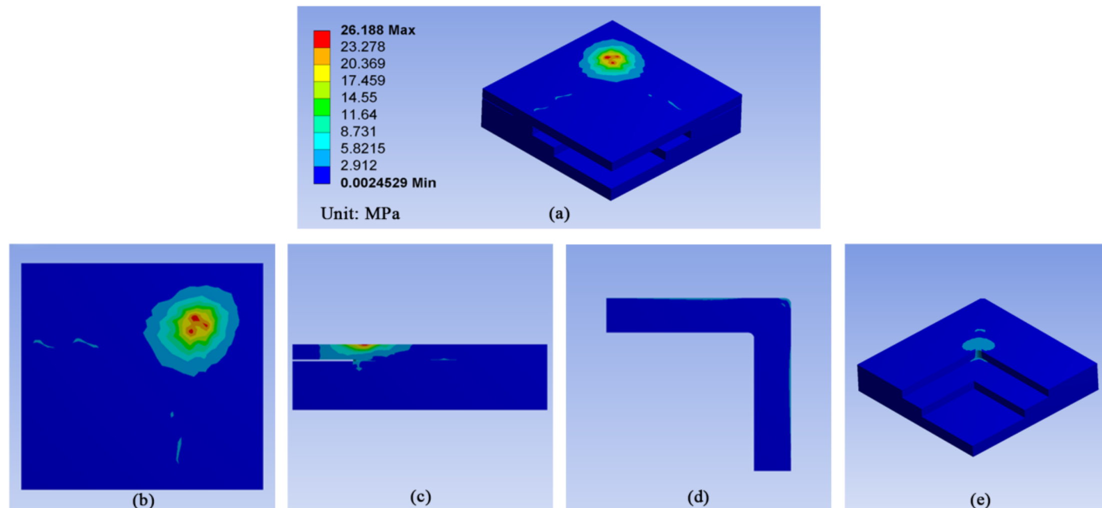

Fig. 5. Stress distribution of Si lid sintered cavity, (a) 3D model, (b) top view of Si lid, (c) cross sectional view of 3D model, (d) top view of sintered Ag layer and (e) 3D view of cavity

Comparing the stress distribution of Cu lid and Si lid sintered cavities, the maximum stress on Cu lid is much higher than that on Si lid. What's more, the stress distribution area on Cu lid is much larger than the Si lid. Since the Cu lid has a lower Young's modulus and a higher CTE than the Si lid, it is more easily to deform, especially when sintering at 250°C. When cooling down, the recovery of the central part of Cu lid is constrained by the sintered Ag layer and causes the high stress distribution, especially at the two sides of the sintered layer. The high stress level and large stress distribution area on Cu lid will lead to the delamination of sintered Ag layer. Therefore, the Si lid is more suitable for the nanosilver sintered hermetic cavities. Additional simulation works have been done to investigate how the sintering pressure affects the stress distribution on lid.

3.3 Effects of sintering pressure on the stress distribution of lid

The sintering pressure can help the sintered Ag layer to get a dense microstructure by increasing the contact area among Ag particles [30, 31]. At the meantime, the sintering pressure will also introduce residual stress and deformation into lid. Fig. 6 shows the stress distribution of Cu lid under various sintering pressures. With the increase of sintering pressure from 5 to 30 MPa, the stress distribution areas on Cu lid are almost the same. The stress has already reached 196.48 MPa even when sintered at 5 MPa. Since the applied pressure is much lower than the generated stress on lid, so the sintering pressure will not greatly affect the stress on lid.

However, the stress distribution areas on Si lid are mainly locates at the corner area of sintered Ag layer, as shown in Fig. 7. The distribution edge of stress on Si lid tends to stretch along the sintered Ag layer. Once the sintering pressure increases to 30 MPa, the stress distributes around the whole sintered Ag layer area on the Si lid. The maximum stress increases from 18.57 MPa to 67.02 MPa when sintering pressure increases from 5 MPa to 30 MPa.

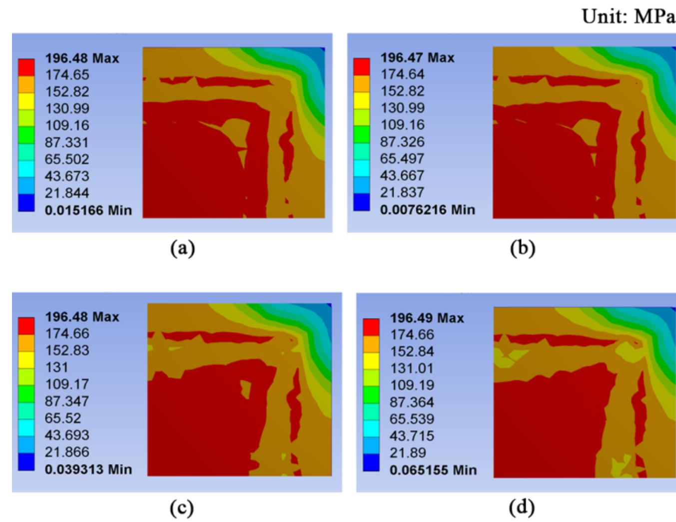

Fig. 6. Effects of sintering pressure on the stress distribution of Cu lid
(a) 5 MPa, (b) 10 MPa, (c) 20 MPa, (d) 30 MPa

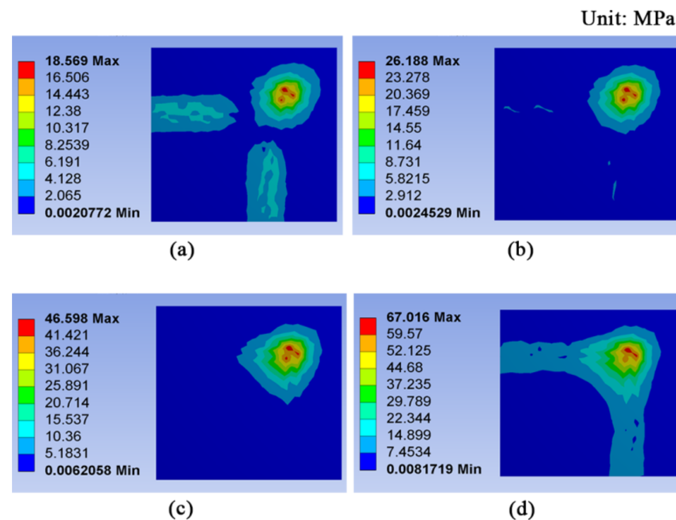

Fig. 7. Effects of sintering pressure on the stress distribution of Si lid
(a) 5 MPa, (b) 10 MPa, (c) 20 MPa, (d) 30 MPa

The maximum stresses on Cu lid and Si lid after sintering at various pressures are shown in Fig. 8. With the increase of sintering pressure from 5 to 30 MPa, the stress on Cu lid is nearly the same, but the stress on Si lid shows increasing trend. The maximum stress on Cu lid is much higher than that on Si lid at each sintering pressure. The high stress on Cu lid will decrease the bonding quality of sintered Ag layer and finally cause the delamination of sintered Ag layer.

Since the Si lid has a lower CTE and a higher Young's modulus than Cu lid, therefore, less deformation and stress will be generated during sintering and cooling process. With the increase of sintering pressure, the deformation of Si lid increases accordingly. The increased deformation of Si lid will further lead to the increase of stress.

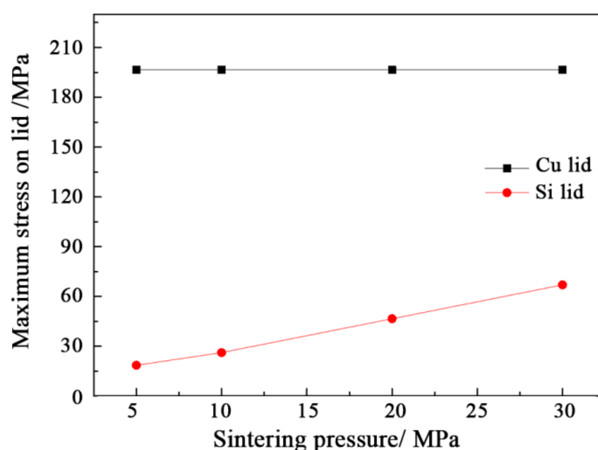

Fig. 8. Effects of sintering pressure on stress distribution of lid

4. Conclusions

The Cu lid and Si lid can be bonded with ceramic cavity by using nanosilver sintering technology. However, delamination was found in Cu lid sintered cavity. The Si lid sintered cavity showed good bonding quality and no crack or delamination was detected. After sintering at 10 MPa, the maximum stress areas on Cu lid are mainly located at the central part of lid. While the maximum stress areas on Si lid are located on the top surface of lid and the outer corner area of the sintered Ag layer. However, the Cu lid has a much higher maximum stress than Si lid. There is no significant change in the stress distribution areas on Cu lid with pressure increasing. However, the stress mainly distributes around the corner area of sintered Ag layer on Si lid when the sintering pressure is below 20 MPa. Comparing with the maximum stresses on Cu lid, the maximum stresses on Si lid show increasing trend with the increase of sintering pressure from 5 to 30 MPa.

Acknowledgement

The work described in this paper was partially supported by the National High-Tech Research and Development Program of China (863 Program) (No. 2015AA033304). National Natural Science Foundation of China (No. 51604090), and Natural Science Foundation of Heilongjiang Province (No. E2017050).

We thank Francois Le Henaff for the assistance of experiments.

References

[1] K. Au, D.M. Zhi, V. Chidambaram, B. Lin, K. Piotr, C. KaiLiang, High temperature endurable hermetic sealing material selection and reliability comparison for IR gas sensor module packaging, Electronics Packaging Technology Conference (EPTC), 2016 IEEE 18th, IEEE, 2016, pp. 1-5.

[2] D.R.M. Woo, J.A.K. Yun, Y. Jun, E.W.L. Ching, F. Che, Extremely high temperature and high pressure (x-HTHP) endurable SOI device & sensor packaging for deep sea, oil and gas applications, Electronics Packaging Technology Conference (EPTC), 2014 IEEE 16th, IEEE, 2014, pp. 16-21.

[3] P. Hagler, P. Henson, R.W. Johnson, Packaging technology for electronic

applications in harsh high-temperature environments, IEEE Transactions on Industrial Electronics, 58(7), 2011, pp. 2673-2682.
[4] L. Chen, G.W. Hunter, P.G. Neudeck, G.M. Beheim, D.J. Spry, R.D. Meredith, Packaging technologies for high temperature electronics and sensors, International Instrumentation Symposium and Machinery Failure Prevention Technology (MFPT) 2013 Joint Conference 59th, 2013, 20130013849.
[5] A.K. Panigrahi, T. Ghosh, S.R.K. Vanjari, S.G. Singh, Demonstration of sub 150 °C Cu-Cu thermocompression bonding for 3D IC applications, utilizing an ultra-thin layer of Manganin alloy as an effective surface passivation layer, Materials Letters, 194, 2017, pp. 86-89.
[6] M.V. Taklo, K. Schjolberg-Henriksen, N. Malik, E. Poppe, S. Moe, T. Finstad, Al-Al wafer-level thermocompression bonding applied for MEMS, Low Temperature Bonding for 3D Integration (LTB-3D), 2017 5th International Workshop on, IEEE, 2017, 16964250.
[7] C. Liu, H. Hirano, J. Froemel, S. Tanaka, Wafer-level vacuum sealing using AgAg thermocompression bonding after fly-cut planarization, Sensors and Actuators A: Physical, 261, 2017, pp. 210-218.
[8] Z. Wu, J. Cai, Q. Wang, J. Wang, D. Wang, Wafer-Level Hermetic Package by Low-Temperature Cu/Sn TLP Bonding with Optimized Sn Thickness, Journal of Electronic Materials, 46(10), 2017, pp. 6111-6118.
[9] V. Vuorinen, A. Rautiainen, H. Heikkinen, M. Paulasto-Kröckel, Optimization of contact metallizations for reliable wafer level Au Sn bonds, Microelectronics Reliability, 64, 2016, pp. 676-680.
[10] L.C. Wai, V.C. Nachiappan, S. Wickramanayaka, C. Oetzel, Chip to wafer hermetic bonding with flux-less reflow oven, Electronics Packaging Technology Conference (EPTC), 2016 IEEE 18th, IEEE, 2016, pp. 38-42.
[11] Y. Li, Y. Xiao, W. Wang, L. Yin, J. Zhang, Effect of the viscosity of organic carrier on the quality of laser-assisted glass frit bonding, Electronic Packaging Technology (ICEPT), 2016 17th International Conference on, IEEE, 2016, pp. 1146-1150.
[12] C. Zhao, J. Wang, S.M. Zhang, J.B. Zou, Glass frit as a hermetic joining material for bonding among three wafers with metallic film feed-through, Key Engineering Materials, 2014, pp. 489-494.
[13] J. Wang, X. He, X. Li, Y. En, X. Zhang, Hermetic packaging of Kovar alloy and low-carbon steel structure in hybrid integrated circuit (HIC) system using parallel seam welding process, Electronic Packaging Technology (ICEPT), 2014 15th International Conference on, IEEE, 2014, pp. 347-351.
[14] X. Hu, M. Bauscher, P. Mackowiak, Y. Zhang, O. Hoelck, H. Walter, M. Ihle, S. Ziesche, U. Hansen, S. Maus, Characterization of anodic bondable LTCC for wafer-level packaging, IEEE Electronics Packaging Technology Conference, 2016, pp. 501-505.
[15] X. Wang, Q. Xu, D. Xiao, Z. Hou, Z. Chen, X. Wu, Vertical signal feedthrough for sandwich devices based on anodic bonding and after laser trimming, Inertial Sensors and Systems, 2016 IEEE International Symposium on, IEEE, 2016, pp.

81-84.
[16] A. Rautiainen, H. Xu, E. Österlund, J. Li, V. Vuorinen, M. Paulasto-Kröckel, Microstructural Characterization and Mechanical Performance of Wafer-Level SLID Bonded Au-Sn and Cu-Sn Seal Rings for MEMS Encapsulation, Journal of Electronic Materials, 44(11), 2015, pp. 4533-4548.
[17] H. Xu, V. Vuorinen, H. Dong, M. Paulasto-Kröckel, Solid-state reaction of electroplated thin film Au/Sn couple at low temperatures, Journal of Alloys & Compounds, 619, 2015, pp. 325-331.
[18] L. Zhang, B. Jiao, W. Ku, L.-T. Tseng, Y. Kong, Y.-H. Chien, S. Yun, D. Chen, An electrical test method for quality detecting of wafer level eutectic bonding, Journal of Micromechanics and Microengineering, 27(1), 2016, 015028.
[19] E.C. Demir, M.M. Torunbalci, I. Donmez, Y.E. Kalay, T. Akin, Fabrication and characterization of gold-tin eutectic bonding for hermetic packaging of MEMS devices, Electronics Packaging Technology Conference (EPTC), 2014 IEEE 16th, IEEE, 2014, pp. 241-245.
[20] F. Arabi, L. Theolier, D. Martineau, J.-Y. Deletage, M. Medina, E. Woirgard, Power electronic assemblies: Thermo-mechanical degradations of gold-tin solder for attaching devices, Microelectronics Reliability, 64, 2016, pp. 409-414.
[21] T.C. Chiu, K.L. Lin, Current induced rapid phase transformation in Au/Sn reaction couple, Journal of Alloys and Compounds, 712, 2017, pp. 111-120.
[22] S.Y. Zhao, X. Li, Y.H. Mei, G.Q. Lu, Study on high temperature bonding reliability of sintered nano-silver joint on bare copper plate, Microelectronics Reliability, 55(12), 2015, pp. 2524-2531.
[23] S.A. Paknejad, S.H. Mannan, Review of silver nanoparticle based die attach materials for high power/temperature applications, Microelectronics Reliability, 70, 2017, pp. 1-11.
[24] C. Weber, H. Walter, M.V. Dijk, M. Hutter, O. Wittler, K.D. Lang, Combination of experimental and simulation methods for analysis of sintered ag joints for high temperature applications, Electronic Components and Technology Conference, 2016, pp. 1335-1341.
[25] L. Xu, M. Wang, Y. Zhou, Z. Qian, S. Liu, An optimal structural design to improve the reliability of Al_2O_3–DBC substrates under thermal cycling, Microelectronics Reliability, 56(6), 2016, pp. 101-108.
[26] L. Xu, Y. Liu, S. Liu, Modeling and simulation of power electronic modules with microchannel coolers for thermo-mechanical performance, Microelectronics Reliability, 54(12), 2014, pp. 2824-2835.
[27] P. Altieri-Weimar, W. Yuan, E. Annibale, S. Schoemaker, D. Amberger, M. Göken, H. Höppel, Reliability model of LED package regarding the fatigue behavior of gold wires, Thermal, Mechanical and Multi-Physics Simulation and Experiments in Microelectronics and Microsystems (EuroSimE), 2016 17th International Conference on, IEEE, 2016, pp. 1-6.
[28] F. Le Henaff, S. Azzopardi, E. Woirgard, T. Youssef, S. Bontemps, J. Joguet, Lifetime Evaluation of Nanoscale Silver Sintered Power Modules for Automotive Application Based on Experiments and Finite-Element Modeling, IEEE

Transactions on Device and Materials Reliability 15(3), 2015, pp. 326-334.
[29] Y. Wang, W. Zhao, M. Li, M. Chen, L. Gao, A simulation of intelligent power module under power cycling condition, Electronic Packaging Technology (ICEPT), 2014 15th International Conference on, IEEE, 2014, pp. 1015-1020.
[30] T.G. Lei, J.N. Calata, G.Q. Lu, X. Chen, S. Luo, Low-Temperature Sintering of Nanoscale Silver Paste for Attaching Large-Area (> 100 mm^2) Chips, IEEE Transactions on Components and Packaging Technologies, 33(1), 2010, pp. 98-104.
[31] Z. Zhang, G. Q. Lu, Pressure-assisted low-temperature sintering of silver paste as an alternative die-attach solution to solder reflow, IEEE Transactions on electronics packaging manufacturing, 25(4), 2002, pp. 279-283.